Experimental Animals
Exp. Anim. 70(2), 257–263, 2021

Original

A reproducible swine model of a surgically created saccular thoracic aortic aneurysm

Soichiro FUKUSHIMA[1,2], Takao OHKI[1], Makoto KOIZUMI[3], Hiroki OHTA[1,2], Toshiki TAKAHASHI[2,4] and Hirotaka James OKANO[2]

[1]*Division of Vascular Surgery, Department of Surgery, The Jikei University School of Medicine, 3-25-8 Nishi-Shinbashi, Minato, Tokyo 105-8461, Japan*
[2]*Division of Regenerative medicine, Research Center for Medical Sciences, The Jikei University School of Medicine, 3-25-8 Nishi-Shinbashi, Minato, Tokyo 105-8461, Japan*
[3]*Laboratory Animal Facilities, The Jikei University School of Medicine, 3-25-8 Nishi-Shinbashi, Minato, Tokyo 105-8461, Japan*
[4]*The Brown University, 75 Waterman St., Providence, RI 02912, USA*

Abstract: A reproducible swine thoracic aortic aneurysm (TAA) model is useful for investigating new therapeutic interventions. We report a surgical method for creating a reproducible swine saccular TAA model. We used eight female swine weighing 20–25 kg (LWD; ternary species). All procedures were performed under general anesthesia and involved left thoracotomy. Following aortic cross-clamping, the thoracic aorta was surgically dissected and the media and intima were resected, and the dissection plane was extended by spreading the outer layer for aneurysmal space. Subsequently, only the adventitial layer of the aorta was sutured. At 2 weeks after these procedures, angiography and computed tomography were performed. After follow-up imaging, the model animals were euthanized. Macroscopic, histological, and immunohistological examinations were performed. All model animals survived, and a saccular TAA was confirmed by follow-up imaging in all cases. The mean length of the shorter and the longer aortic diameter after the procedure were 14.01 ± 1.0 mm and 18.35 ± 1.4 mm, respectively (P<0.001). The rate of increase in the aortic diameter was 131.7 ± 13.8%, and the mean length of aneurysmal change at thoracic aorta was 22.4 ± 1.9 mm. Histological examination revealed intimal tears and defects of elastic fibers in the media. Immunostaining revealed MMP-2 and MMP-9 expressions at the aneurysm site. We report our surgical method for creating a swine saccular TAA model. Our model animal may be useful to investigate new therapeutic interventions for aortic disease.
Key words: surgical method, swine saccular thoracic aortic aneurysm

Introduction

Endovascular aortic aneurysm repair (EVAR) is a less invasive treatment option for life threatening aortic disease. We previously reported the clinical outcomes of endovascular repair for aortic disease including aortic dissection, and complex aortic aneurysms [1, 2]. However, we sometimes experience an additional treatment even after EVAR, caused by an endoleak (EL), endograft infection, or endograft material deterioration [3–5]. For further treatment improvement, a reproducible large animal aortic disease model is required for investigating new therapeutic device and interventions.

Many methods for creating aortic disease large animal model have been previously reported. Fujii *et al.* attempted to surgically create a thoracic aortic dissection model using 12 swine [6]. They found that an aortic dissection model could be created in swine; however, they concluded that the use of aortic cross-clamping and pentobarbital should be avoided since it leads to a low

(Received 10 September 2020 / Accepted 27 December 2020 / Published online in J-STAGE 10 February 2021)
Corresponding authors: T. Ohki. e-mail: takohki@msn.com/ H.J. Okano. e-mail: hjokano@jikei.ac.jp

animal survival rate. Okuno *et al.* reported a minimally invasive method for swine aortic dissection model creation using a transcatheter technique, which does not require an invasive step including aortic cross-clamping [7]. However, a patent chronic dissected aortic aneurysm was successfully created in only 5 out of 14 cases. A vein patch method is known as one of a method for creating an aortic aneurysm animal model [8, 9]; however, it requires an invasive step for harvesting patch materials, in addition, the created aneurysm wall is composed of veins, which is never been treated in daily human clinical practice.

In this study, we establish a surgical method for creating a reproducible swine saccular thoracic aortic aneurysm (TAA) model without patch materials. Here, we report our new surgical method.

Material and Methods

The protocol of animal experiments was reviewed and approved by the Institutional Animal Care and Use Committee of our institute, and it conformed to the Guidelines for the Proper Conduct of Animal Experiments of the Science Council of Japan (2006). As experimental animals, we used a ternary species (LWD; female swine weighing 20–25 kg).

The surgical method for creating a swine saccular TAA model was performed in eight swine. First, medetomidine (0.05 mg/kg) and midazolam (0.2 mg/kg) were intramuscularly injected into the animals to achieve mild sedation. Then, endotracheal intubation was performed, and general anesthesia was introduced with isoflurane 3–5% inhalation. After the introduction of general anesthesia, we surgically exposed the common carotid artery, and an arterial pressure monitoring line was placed into the artery. We monitored the arterial blood pressure during the procedure including cross-clamping at thoracic aorta.

Subsequently, the position was changed to right lateral position, and the region from the distal arch to the descending aorta was exposed via a left 4–5th intercostal thoracotomy. In order to control back bleeding during aortotomy, one or two pairs of the intercostal artery were ligated and separated. Following these surgical steps, preprocedural computed tomography (CT) scan for acquiring the baseline data of aorta was performed. After CT imaging, heparin (200 U/kg) was intravenously injected, and then, the surgical creation of the saccular TAA was performed.

During the aortic procedure, we performed the following three steps before aortic cross-clamping in attempt to reduce the aortic cross-clamping time. First, we incised only the outer layer of the thoracic aorta approximately 1/3 round without aortic cross-clamping. Second, we bluntly detached the space under the incised membrane. Third, we sutured both edges of the incised adventia with 6-0 Prolene (Ethicon, Somerville, NJ, USA) to shorten the subsequent aortic clamping time. Subsequently, the thoracic aorta was clamped. During aortic cross-clamping, the inhalation anesthetic concentration was adjusted for a systolic blood pressure ≤120 mmHg to avoid excessive cardiac afterload.

During aortic cross-clamping, the aortic media and intima were resected into a spindle shape of about 10 mm at the site where the outer layer was incised, and an aortic dissected entry tear was surgically created (Fig. 1a). After the intima was excised, only the adventitial layer was sutured and closed using the 6-0 Prolene (Ethicon) sutures that had been previously placed (Fig. 1b). After these surgical steps, aortic cross-clamping was carefully released. Following the above procedures, the left thoracic cavity was irrigated with physiological saline and closed. A chest drain for postoperative management was not placed.

At 2 weeks after these procedures, follow-up angiog-

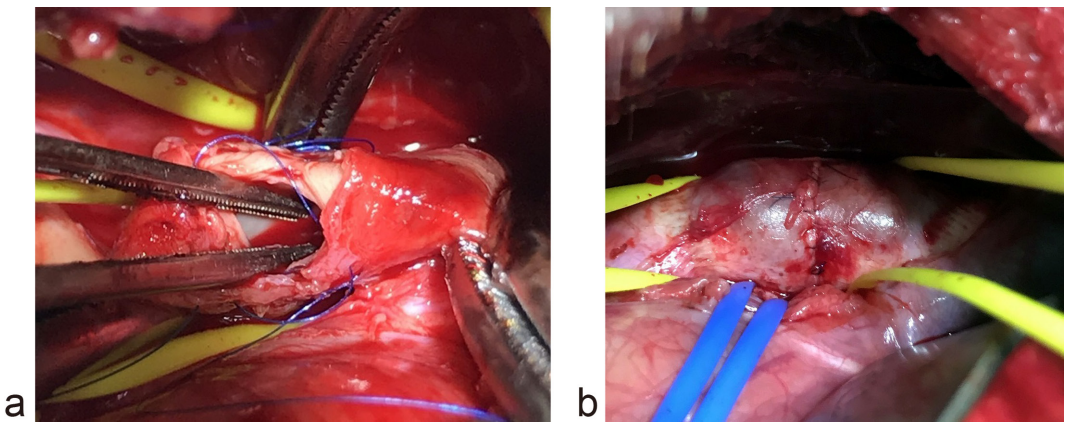

Fig. 1. a. Surgical creation of a primary tear at the thoracic aorta. b. Aneurysm formation at the thoracic aorta.

 doi: 10.1538/expanim.20-0142

raphy and CT were performed under general anesthesia (Figs. 2a–c.). Aortic diameter, aneurysmal length at thoracic aorta was measured by angiographic and CT imaging. Aortic aneurysm volume was also measured by CT using Aquarius iNtuition® (Terarecon, Inc., Foster City, CA, USA) imaging software. After follow-up imaging, the animals were euthanized. The thoracic aorta was harvested, and gross and histological findings were assessed.

Histological findings were assessed using hematoxylin and eosin stain (H&E stain), Masson trichrome stain (Masson stain), and Elastica van Gieson stain (EVG stain). For verifying the expressions of MMP-2 and MMP-9 which are well known proteins as characteristic markers as aortic aneurysm pathology in the treated aorta, excised aortic sections were embedded in paraffin, and staining was performed using anti-MMP-2 antibody (PGI Proteintech, Inc., Tokyo, Japan) and anti-MMP-9 antibody (QuickZyme Biosciences, Leiden, the Netherlands).

Data are presented as mean ± SD. The study results were analyzed using GraphPad Prism® version 7.0 (GraphPad Software, San Diego, CA, USA). Differences between the groups were tested using the *t*-test. A *P*-value <0.05 was considered statistically significant.

Results

All animals survived after the surgical procedure. The mean procedure time from skin incision to closure was 180.9 ± 37.4 min. The mean aortic clamping time was 9.6 ± 1.9 min. There was no serious complication associated with the procedure, including embolization, and other ischemic event.

Follow-up angiography and CT performed at 2 weeks after the procedure verified the diagnosis in all animals. A saccular TAA was confirmed in all cases (Fig. 3). The mean shorter and longer aortic diameters after the procedure were 14.01 ± 1.0 mm and 18.35 ± 1.4 mm, respectively (P<0.0001). The rate of increase in the aortic diameter was 131.7 ± 13.8%. The mean length of aneurysmal change at thoracic aorta was 22.44 ± 1.9 mm. The mean aneurysm volume was 1.22 ± 0.5 cm^3. We showed these results in Table 1.

Macroscopic examination of the thoracic aorta re-

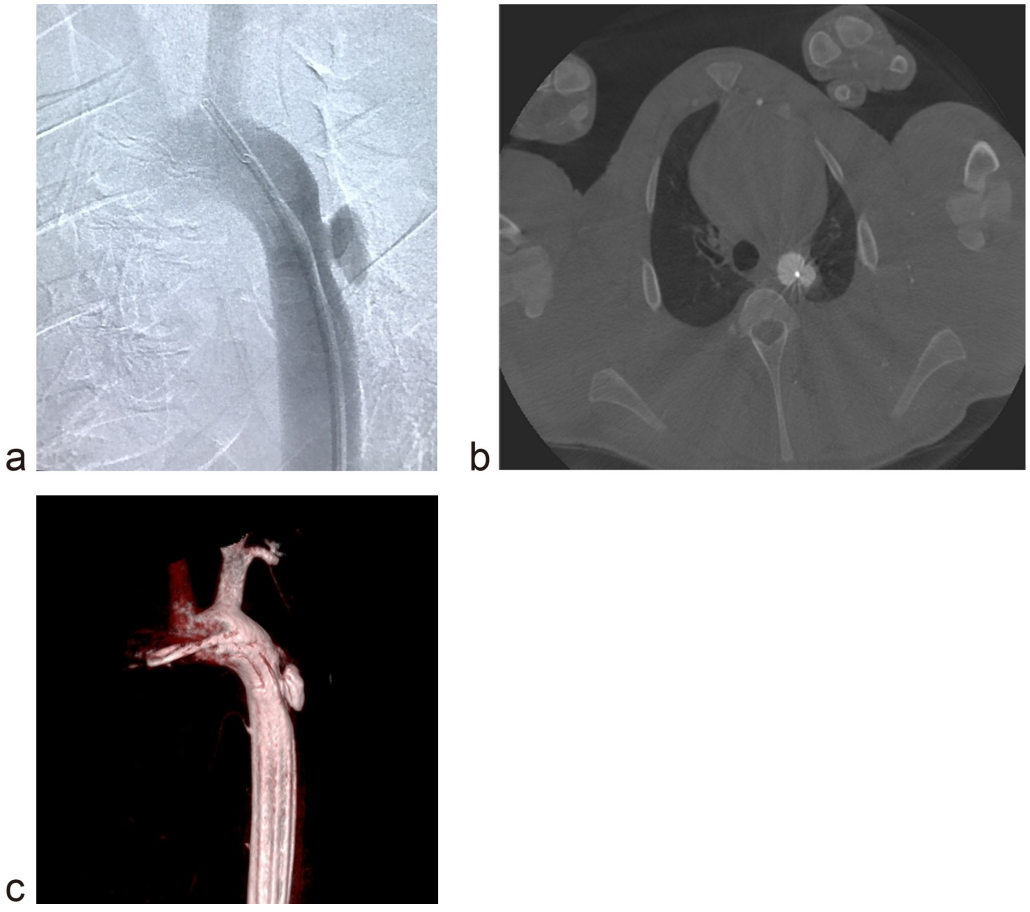

Fig. 2. a. Aortography shows a saccular dissected thoracic aortic aneurysm. b. Computed tomography (CT) shows a patent dissected saccular thoracic aortic aneurysm. c. Three-dimensional CT shows a saccular dissected thoracic aortic aneurysm.

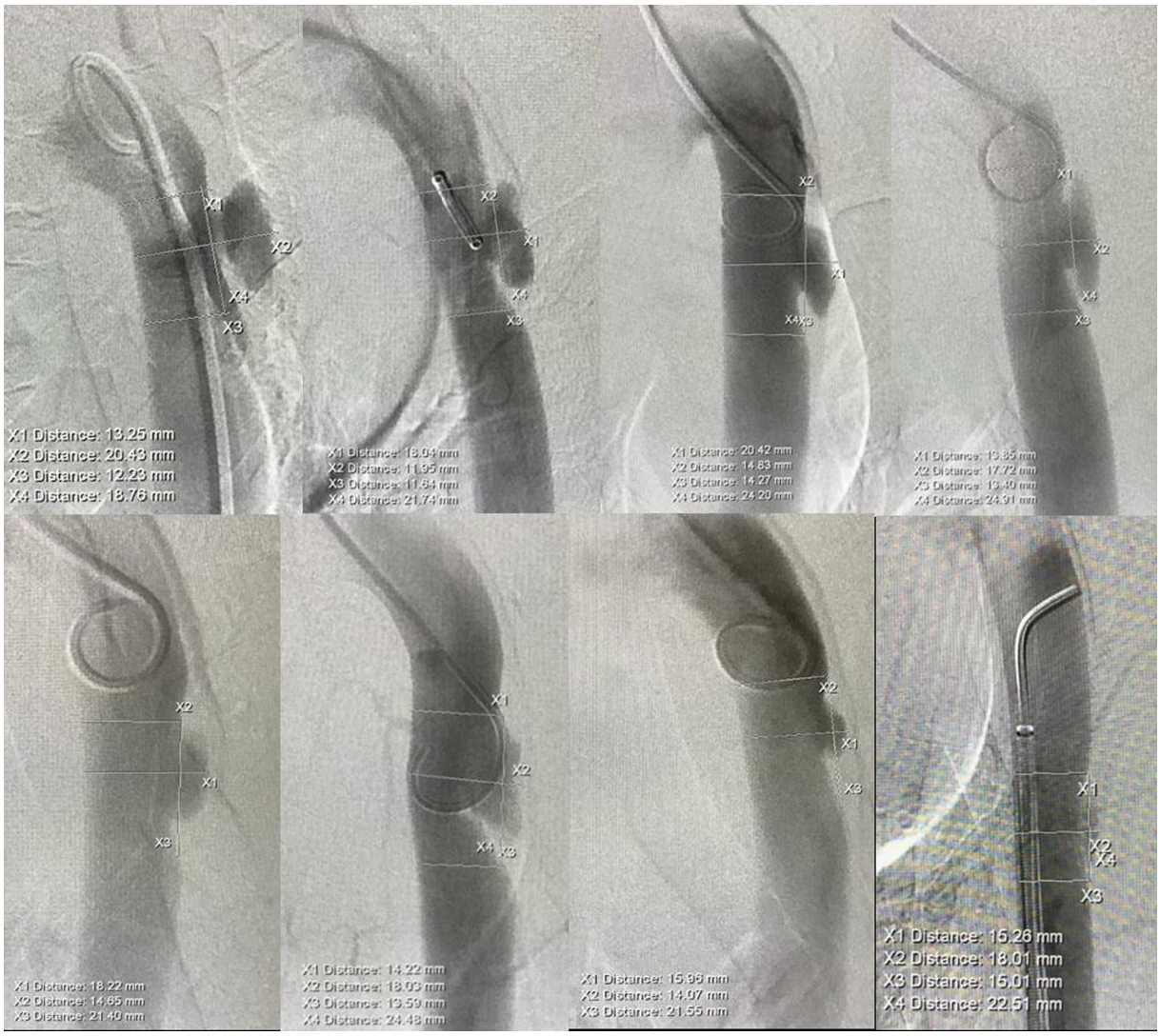

Fig. 3. Angiographic imaging of all saccular TAA model animals.

Table 1. Detailed data of the created aneurysm

	Pre (mm)	Post (mm)	Dilation (%)	Length (mm)	Volume (mm^3)
Case 1	13.25	20.43	154.18	18.76	1.16
Case 2	13.85	17.72	127.94	24.91	1.08
Case 3	14.83	20.42	137.69	24.2	0.98
Case 4	11.95	18.04	150.96	21.74	1.89
Case 5	14.22	18.03	126.79	24.48	0.85
Case 6	14.07	15.96	113.43	21.55	1.82
Case 7	14.65	18.22	124.37	21.4	1.61
Case 8	15.26	18.01	118.02	22.51	0.35
Mean ± SD	14.01 ± 1.0	18.35 ± 1.4	131.67 ± 13.8	22.44 ± 1.9	1.22 ± 0.5

vealed a sac-like aortic aneurysm localized at the intervention site, and a surgically created the dissected entry tear was confirmed on the intimal side (Fig. 4a).

Histological examination with H&E stain and EVG stain at the same site confirmed intimal defects and cracks in the medial elastic fibers at the dissected entry tear site, where the intervention was performed in all cases. Examination with Masson trichrome stain showed greater thickening of collagen fibers in the outer layer at the intervention area than at the non-intervention area. Infiltration of inflammatory cells and calcification in the aneurysm wall, which were often observed in fusiform aortic aneurysm, were not observed in our disease model.

According to these histological findings, the aneurysm in our disease model was considered consistent with a saccular TAA. We show these examination findings in-

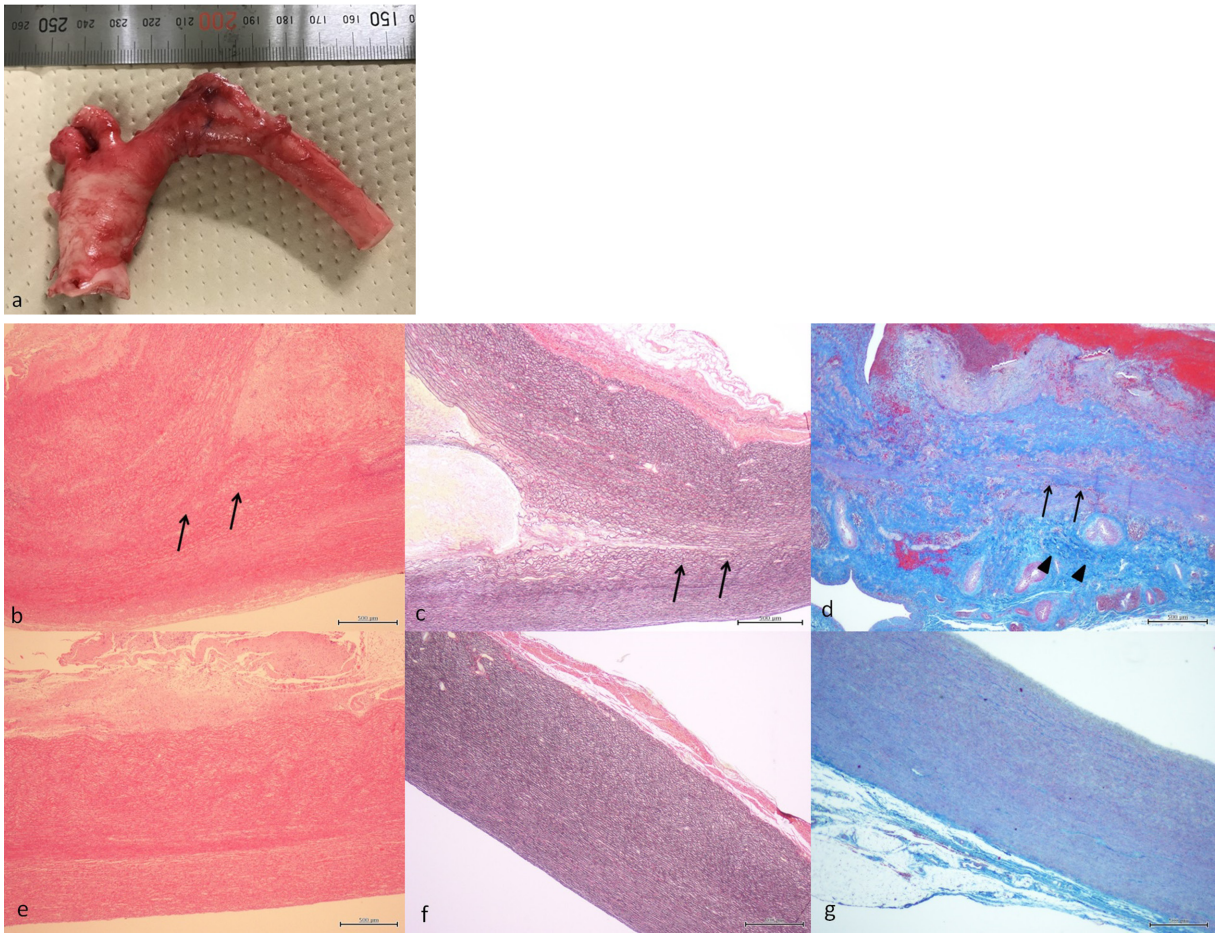

Fig. 4. a. Macroscopic examination shows the aneurysmal change at thoracic aorta. b. Histological examination with H&E stain (×40) shows intimal defects and cracks in the medial elastic fibers at the entry site. Arrows indicate breakage of elastic fibers at the middle layer of the aorta (Scale bar=500 μm). c. Histological examination with EVG stain (×40) shows intimal defects and cracks in the medial elastic fibers at the entry site. Arrows indicate breakage of elastic fibers at the middle layer of the aorta (Scale bar=500 μm). d. Histological examination with Masson trichrome stain (×40) shows greater thickening of collagen fibers in the outer layer at the intervention area than at the non-intervention area. Arrows (↑) indicate breakage of elastic fibers at the middle layer of the aorta. An arrowhead (▲) indicates hyperplasia of collagenous fibers at the outer layer of the aorta (Scale bar=500 μm). e. Histological examination of healthy aorta with H&E stain (×40) (Scale bar=500 μm). f. Histological examination of healthy aorta with EVG stain (×40) (Scale bar=500 μm). g. Histological examination of healthy aorta with Masson trichrome stain (×40) (Scale bar=500 μm).

cluding healthy controls in Figs. 4b–g.

Immunostaining (anti-MMP-2 and anti-MMP-9 antibodies) of the thoracic aorta where the intervention was performed showed expressions of both MMP-2 (Figs. 5a–d) and MMP-9 (Figs. 5e–h) at the dissected aneurysm site. Although MMP-9 expression was not prominent at the intervention site, MMP-2 was markedly expressed in both the intima and adventitia confirming the presence of degenerative changes. We show the examination findings of healthy controls in Figs. 5i–k.

Discussion

Improving the success rate of the surgical procedure

In the creation of disease animal models, high reproducibility is important, but at the same time, minimization of the invasiveness is also important in view of the 3R principle for protecting model animals [10].

In this study, we report a reproducible surgical method involving aortic cross-clamping for creating a saccular TAA model. Thoracic aortic cross-clamping, which has been reported to be unacceptable owing to its high invasiveness [6], results in a poor survival rate of animals. We performed several steps before aortic cross-clamping to reduce the total aortic cross-clamping time, and as a result, we completed our procedure with a short aortic clamping time of 9.6 ± 1.9 min, which probably resulted in high success and survival rate in this study.

Advantages of animal model in this study

The model created in this study has two advantages. First, it is easy for us to evaluate the new treatment re-

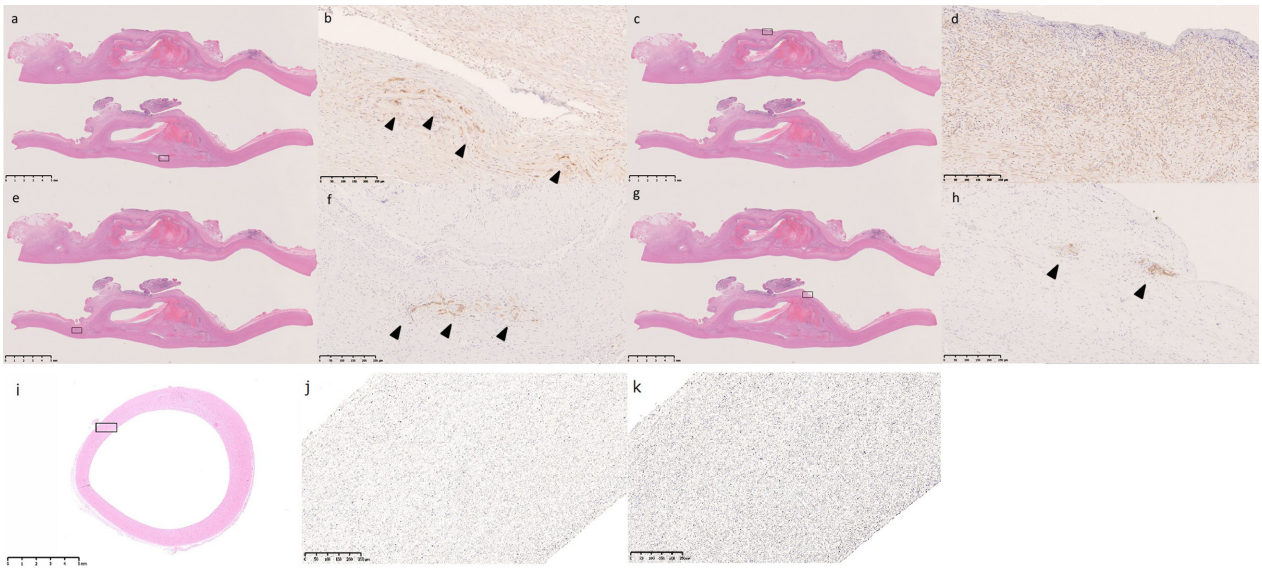

Fig. 5. a, b. Immunostaining of anti-MMP-2 antibodies of the thoracic aorta shows expressions of MMP-2 at the dissected aneurysm site (a: Scale bar=1 mm / b: Scale bar=250 μm). An arrowhead (▲) indicates MMP-2 expression at the inner layer of the dissected aorta. c, d. Immunostaining of anti-MMP-9 antibodies of the thoracic aorta shows expressions of MMP-9 at the dissected aneurysm site (c: Scale bar=1 mm / d: Scale bar=250 μm). Image shows MMP-9 expression at the outer layer of the dissected aorta. e, f. Immunostaining of anti-MMP-9 antibodies of the thoracic aorta shows expressions of MMP-9 at the dissected aneurysm site (e: Scale bar=1 mm / f: Scale bar=250 μm). An arrowhead (▲) indicates MMP-9 expression at the inner layer of the dissected aorta. g, h. Immunostaining of anti-MMP-9 antibodies of the thoracic aorta shows expressions of MMP-9 at the dissected aneurysm site (g: Scale bar=1 mm / h: Scale bar=250 μm). An arrowhead (▲) indicates MMP-9 expression at the outer layer of the dissected aorta. i. Histological examination of normal healthy aorta with H&E stain (×40) (Scale bar=5 mm). j. Immunostaining of anti-MMP-2 antibodies of the healthy thoracic aorta (Scale bar=250 μm). k. Immunostaining of anti-MMP-9 antibodies of the healthy thoracic aorta (Scale bar=250 μm).

sults by angiographic imaging, since the model has a visible saccular TAA. With small fusiform aortic aneurysms, it is difficult for us to evaluate the treatment results by an angiographic imaging. Second, there are no patch materials including veins for aortic aneurysm wall in this model. From this point of view, the model created in this study better mimics an aortic aneurysm treated in daily clinical practice than the aneurysm created by previously reported patch method.

Pathological findings of animal model in this study

MMP-2 and MMP-9 are well known proteins expressed at the inflammation site, which were commonly observed at aortic aneurysm wall. Both proteins are recognized as characteristic markers as aortic aneurysm pathology. In this study, immunostaining (anti-MMP-2 and anti-MMP-9 antibodies) of the thoracic aorta showed expressions of both MMP-2 and MMP-9 at the dissected aneurysm site. The macroscopic and microscopic findings including immunostaining of the thoracic aorta prove that the new model is suitable as a TAA model.

On the other hands, this surgically created new saccular TAA models do not fully reflect human clinical pathology, including atherosclerotic or degenerative most of which manifest as fusiform aortic aneurysm. Such aneurysm shows infiltration of inflammatory cells and calcification in the aneurysm wall; however, these findings were not observed in our disease model. It may reflect the pathological differences between surgically created aortic aneurysms and spontaneous aortic aneurysms. In that respect, our disease model animals are not exactly the same as the aneurysms encountered in human clinical practice.

Therapeutic interventions in disease animal models

Recently, endovascular treatment is recognized as a 1st line treatment option for high risk aortic disease patients. However, there are unresolved problems even after endovascular treatment, including endoleak, endograft infection, and endograft material deterioration. These unsolved issues should be overcome in the future.

The advantage of creating large animal aortic disease model is that we could assess the effectiveness of new therapeutic devices or interventions intended for clinical use in humans, as vessel diameters in these model animals are similar to those in humans. Verification of new treatment devices from an engineering perspective can be performed using an in vitro simulator [11]. However,

in vivo verification using disease model animals is indispensable for the clinical application of new therapeutic devices and for mid- to long-term safety assessment [12]. Furthermore, with regard to aortic diseases, the verification of the repair mechanisms of stem cells in the pathological aortic wall [13] and the possibility of regeneration with intravenous administration of mesenchymal stem cells in a rat abdominal aortic aneurysm model [14] have been reported in recent years. *In vivo* disease animal models are indispensable for the verification of such new treatments, and our reproducible method for creating a TAA model may be useful for verification studies, including those that require post procedural follow-up of the model animals.

Limitations of in this study

In this study, we report a disease animal model creation method of a saccular TAA, which is different from fusiform aortic aneurysm. A saccular TAA is suitable for investigating new endovascular treatment device for aortic disease using angiographic imaging tools; however, other methods should be selected when the investigation for fusiform aneurysm is required [15]. In addition, the disease model animals do not fully reflect human clinical pathology. Even if new treatments for our model animals are successful, careful application is required for human clinical practice.

Conclusions

We reported our surgical method for creating a swine reproducible saccular TAA model, which is associated with a high survival rate. Our swine TAA model can be used to assess novel therapeutic devices and interventions.

Conflict of Interest

Dr. Takao Ohki is a paid consultant for W.L. Gore & Associates. The other authors declare that they have no conflict of interest.

Funding

This research was supported by The Jikei University Research Fund for Graduate Students and the Department of surgery, division of vascular surgery.

Acknowledgment

We would like to thank Y. Minowa and S. Ogatsu for their dedicated support of laboratory animal care.

References

1. Fukushima S, Ohki T, Toya N, Shukuzawa K, Ito E, Murakami Y, et al. Initial results of thoracic endovascular repair for uncomplicated type B aortic dissection involving the arch vessels using a semicustom-made thoracic fenestrated stent graft. J Vasc Surg. 2019; 69: 1694–1703. [Medline] [CrossRef]
2. Fukushima S, Ohki T, Kanaoka Y, Ohta H, Ohmori M, Momose M. Mid-Term Results of Thoracic Endovascular Aneurysm Repair with Intentional Celiac Artery Coverage for Crawford Type I Thoracoabdominal Aortic Aneurysms with the TX2 Distal Component Endograft. Ann Vasc Surg. 2020; 66: 193–199. [Medline] [CrossRef]
3. Hoshina K, Ishimaru S, Sasabuchi Y, Yasunaga H, Komori K. Japan Committee for Stentgraft Management (JACSM)*. Outcomes of Endovascular Repair for Abdominal Aortic Aneurysms: A Nationwide Survey in Japan. Ann Surg. 2019; 269: 564–573. [Medline] [CrossRef]
4. Shukuzawa K, Ohki T, Maeda K, Kanaoka Y. Risk factors and treatment outcomes for stent graft infection after endovascular aortic aneurysm repair. J Vasc Surg. 2019; 70: 181–192. [Medline] [CrossRef]
5. Murakami Y, Toya N, Fukushima S, Ito E, Akiba T, Ohki T. Aneurysm sac enlargement 16 years after endovascular aortic aneurysm repair due to late type IIIb endoleak: A case report. Int J Surg Case Rep. 2018; 49: 215–218. [Medline] [CrossRef]
6. Fujii H, Tanigawa N, Okuda Y, Komemushi A, Sawada S, Imamura H. Creation of aortic dissection model in swine. Jpn Circ J. 2000; 64: 736–737. [Medline] [CrossRef]
7. Okuno T, Yamaguchi M, Okada T, Takahashi T, Sakamoto N, Ueshima E, et al. Endovascular creation of aortic dissection in a swine model with technical considerations. J Vasc Surg. 2012; 55: 1410–1418. [Medline] [CrossRef]
8. Pavcnik D, Andrews RT, Yin Q, Uchida BT, Timmermans HA, Corless C, et al. A canine model for studying endoleak after endovascular aneurysm repair. J Vasc Interv Radiol. 2003; 14: 1303–1310. [Medline] [CrossRef]
9. Li W, Xu K, Ni Y, Zhong H, Bi Y. A canine model of proximal descending thoracic aortic aneurysm created with an autologous pericardial patch. Ann Thorac Cardiovasc Surg. 2013; 19: 131–135. [Medline] [CrossRef]
10. Russell WM. The development of the three Rs concept. Altern Lab Anim. 1995; 23: 298–304. [Medline] [CrossRef]
11. Rudenick PA, Bijnens BH, García-Dorado D, Evangelista A. An in vitro phantom study on the influence of tear size and configuration on the hemodynamics of the lumina in chronic type B aortic dissections. J Vasc Surg. 2013; 57: 464–474.e5. [Medline] [CrossRef]
12. Kanaoka Y, Ohki T, Huang J, Shah A. A comparison between standard and high density Resilient AneuRx in reducing aneurysm sac pressure in a chronic canine model. J Vasc Surg. 2009; 49: 1021–1028. [Medline] [CrossRef]
13. Shen YH, Hu X, Zou S, Wu D, Coselli JS, LeMaire SA. Stem cells in thoracic aortic aneurysms and dissections: potential contributors to aortic repair. Ann Thorac Surg. 2012; 93: 1524–1533. [Medline] [CrossRef]
14. Hosoyama K, Wakao S, Kushida Y, Ogura F, Maeda K, Adachi O, et al. Intravenously injected human multilineage-differentiating stress-enduring cells selectively engraft into mouse aortic aneurysms and attenuate dilatation by differentiating into multiple cell types. J Thorac Cardiovasc Surg. 2018; 155: 2301–2313.e4. [Medline] [CrossRef]
15. Eckhouse SR, Logdon CB, Oelsen JM, Patel RK, Rice AD, Stroud RE, et al. Reproducible porcine model of thoracic aortic aneurysm. Circulation. 2013; 128:(Suppl 1): S186–S193. [Medline] [CrossRef]